ELSEVIER

Coordination Chemistry Reviews
190–192 (1999) 185–198

COORDINATION CHEMISTRY REVIEWS

www.elsevier.com/locate/ccr

The interaction of ferrocenoyl peptides with 3-aminopyrazole

P. Saweczko, H.-B. Kraatz *

Department of Chemistry, University of Saskatchewan, 110 Science Place, Saskatoon, SK, Canada S7N 5C9

Accepted 17 February 1999

Contents

* Corresponding author. Tel.: +1-306-966-4660; fax: +1-306-966-4730.
E-mail address: kraatz@skyway.usask.ca (H.-B. Kraatz)

PII: S0010-8545(99)00077-6

Abstract

The syntheses of three ferrocenoyl peptides (Fc–GG–OEt (**2**), Fc–AA–OBzl (**3**), Fc–LF–OMe (**4**)) including their full spectroscopic characterization is reported. Titration of peptide solution with 3-aminopyrazole (APzl) in $CDCl_3$ was followed by ^{1}H-NMR spectroscopy and evaluated using Job's method and by non-linear regression. It was found that **4** showed the strongest interaction with APzl, followed by **3**. The highly flexible **2** showed only a weak interaction. Association constants, derived from NMR measurements, are in the range of 9.4 ± 1.0 to 21.4 ± 0.5 M^{-1}. Cyclic voltammetry shows that the redox potentials are sensitive to complex formation. The largest changes were observed for **4** (30 mV), followed by **3** (13 mV) and there was no observable change for **2**. This sequence coincides with the ability of 3-APzl to form a complex with the Fc-peptide.

Keywords: Hydrogen bonding; β-Sheet; Peptide; Binding constants; Ferrocene; Non-linear regression

1. Introduction

The ferrocene group is a sensitive electrochemical probe that has been widely used to detect structural changes taking place upon binding of charged and neutral molecules [1–5]. Recently, we have shown that the redox potential of the ferrocenoyl group (Fc) is influenced by the amino acid substituents [6], and if attached to various peptides, is influenced by the secondary structure of the peptide [7]. According to solid state and solution structures of Fc–P_n–OBzl (P = proline, Pro; $n = 1$–4), these systems exhibit a helical structure typical of polyproline-II, with a repeat unit of ca. 3 prolines per turn. With growing oligoproline chain length, the molecule becomes easier to oxidize. This trend has been attributed to the formation of the polyproline II helix. Once the helix is fully formed, as it is in the case of Fc–P_3–OR and Fc–P_4–OR no further changes in the redox potentials are observed. On the other hand, Fc-peptides having β-turn like structures, Fc–PPF–OH and Fc–PPFA–OH (F = phenylalanine, Phe; A = alanine, Ala) are significantly more difficult to oxidize than the helical systems mentioned above. This may indicate that the formation of other types of secondary structural elements might also influence the redox potential of the Fc group. Thus, as a logical next step, we wanted to include systems that have β-sheet-like structures and study their electrochemical properties.

Recently, several procedures were developed that allowed the de novo design of β-sheet structures [8]. We were intrigued by a novel strategy, recently reported by Kirsten and Schrader [9], using substituted pyrazoles as templates to induce β-sheet formation by forming hydrogen bonds with the peptide backbone. In experimental studies using acylated dipeptides, it was shown that 3-aminopyrazole (APzl) and other derivatives are able to H-bond to the peptide backbone in two distinct binding modes (Scheme 1). It was shown that dipeptides possess two faces, distinguishable by the number of hydrogen-bonding sites.

The top face was defined as possessing a binding site able to establish three hydrogen bonds with a substrate, whereas the bottom face can only establish two H-bonds. It was found that the top face strongly interacts with APzl, thereby making it possible to distinguish it from the weaker interaction of the bottom face of the peptide. Hence, the three-point site will be occupied preferentially over the bottom two-point binding site.

We decided to make use of this strategy for our purposes and investigate the electrochemical response of the Fc moiety to the presence of the APzl substrate. For this purpose, we had to study the coordination behavior of APzl with the Fc peptides and establish that the β-sheet conformation is indeed adopted. Electrochemical studies of these systems can then be compared to non-β-sheet systems. This approach may allow us to investigate how the β-sheet conformation affects the electrochemistry of the Fc moiety. In this paper, we will report our findings on the interaction of simple Fc-peptides with APzl and report their electrochemical behavior.

2. Experimental section

2.1. General procedure

CH_2Cl_2 and $CHCl_3$ (ACS grade; BDH) used for the purposes of synthesis and electrochemistry were dried over CaH_2 and freshly distilled prior to use. Pyrazole and 3-aminopyrazole (Aldrich) were used as received. Coupling reagents 1,3-dicyclohexylcarbodimide (DCC) and 1-hydroxybenzotriazole hydrate (HOBt) (Aldrich) were used as received. H–Gly–OEt·HCl, H–Phe–OMe·HCl (Aldrich), H–Ala–Obzl-*p*-tosylate, Boc–Gly–OH, Boc–Leu–OH·H_2O, Boc–Ala–OH (Novabiochem) and Boc–Phe–OH (AminoTech) were used as received. Peptide couplings and ferrocenoyl-peptide syntheses were carried out in air. $CDCl_3$ (Aldrich) was stored over molecular sieves (8–12 mesh; 4 Å effective pore size; Fisher). Ferrocene carboxylic acid was prepared according to the procedure of Goldberg et al. [10].

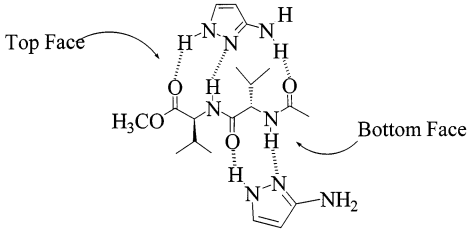

Scheme 1. Interaction of 3-aminopyrazole (APzl) with a N,C-protected dipeptide (Ac–V_2–OMe). First one APzl molecule makes three cooperative H-bonds with the top face of divaline, then a second APzl molecule interacts with the bottom face of the dipeptide in a two-point binding manner [9].

^{1}H- and ^{13}C{^{1}H}-NMR were recorded on a Bruker AMX-300 at 300.135 and 75.478 MHz,, respectively. ^{1}H- and ^{13}C{^{1}H}-NMR spectra are reported in ppm relative to tetramethylsilane and are referenced to the residual signal of $CHCl_3$ (δ 7.27) for ^{1}H-NMR and the $CDCl_3$ signal (δ 77.23) for ^{13}C{^{1}H}-NMR. 2D-COSY and HMBC (heteronuclear multiple bond correlation) experiments were used to make assignments in the ^{1}H- and ^{13}C-NMR spectra.

2.2. Peptide coupling: Boc–LF–OMe

To the Boc–Leu–OBt active ester, prepared in situ from Boc–Leu–OH (0.249 g, 1 mmol), HOBt (0.149 g, 1.1 mmol) and DCC (0.227 g, 1.1 mmol) in CH_2Cl_2 (10 ml, 0°C), a solution of freshly prepared H–Phe–OMe, obtained by treatment of H–Phe–OMe·HCl (0.237 g, 1.2 mmol) with Et_3N (1.2 ml) in CH_2Cl_2 (6 ml), was added. After 12 h, dicyclohexylurea (DCU) was removed by filtration through a cotton pad. The filtrate was treated consecutively with aqueous solutions of $NaHCO_3$ (sat.), citric acid (10%), and $NaHCO_3$ (sat.), and finally with H_2O. The organic phase was dried over anhydrous $MgSO_4$, filtered through a cotton pad and evaporated to dryness, giving a white solid, which was redissolved in CH_2Cl_2 (2 ml), filtered through cotton, and allowed to evaporate in air. This purification step was repeated until all the DCU byproduct was removed. Yield: 96%. MW for $C_{21}H_{32}N_2O_5$: Anal. Calc. 392.5; Found 393.2 $[M+1]^+$. ^{1}H-NMR (δ ppm, $CDCl_3$): 7.28 (3H, m, *m*- and *p*-C*H* F); 7.11 (2H, d, $J = 6.3$ Hz, o-C*H* F); 6.51 (1H, d, $J = 7.8$ Hz, N*H* F); 4.84 (2H, m, C*H* L and F); 4.08 (1H, br. s, NH L); 3.72 (3H, s, O–CH_3); 3.13 (2H, complex multiplet, CH_2 F); 1.64 (1H, m, $CH_2CH(CH_3)_2$ L); 1.44 (11H, br. s, $CH_2CH(CH_3)_2$ L (2H) and Boc group (9H)); 0.91 (6H, m, $CH_2CH(CH_3)_2$ L).

2.3. General procedure: ferrocenoyl peptides

To a mixture of ferrocene carboxylic acid (1 mmol) and HOBt (1.1 mmol) in CH_2Cl_2 (20 ml) at room temperature, solid DCC (1.1 mmol) is added. DCU begins to precipitate from the reaction mixture after 10–15 min. Boc-protected peptide (1.2 mmol) is treated with TFA (1 ml) for 30 min, after which excess TFA is removed under a stream of argon. The residue is dissolved in CH_2Cl_2 (5 ml), Et_3N (1 ml) is added, and the peptide solution transferred to the stirring reaction mixture, which is stirred overnight. DCU is removed by filtration through a cotton plug (1 cm) and the filtrate washed consecutively with saturated $NaHCO_3$, citric acid (10%), $NaHCO_3$ and lastly with water. The organic phase is dried over $MgSO_4$. After filtration, the solution is evaporated under reduced pressure giving the crude product. After DCU impurities are removed by the same method described for Boc-protected peptides, yellow to orange-red ferrocenoyl-peptides are obtained in moderate yield.

2.4. Spectroscopic characterization

2.4.1. Spectroscopic data for Fc–G_2–OEt (**2**)

Yield: 59%. IR (cm^{-1}, KBr, film): 1746 (C=O). Elemental analysis for $C_{17}H_{20}FeN_2O_4$: Anal. Calc. C, 54.86; H, 5.42; N, 7.53. Found C, 54.69; H, 5.20; N, 7.45. EI-MS: Accurate mass for $C_{17}H_{20}FeN_2O_4$: Anal. Calc. 372.0772. Found, 372.0776 $[M]^+$. ^{1}H-NMR (δ in ppm, $CDCl_3$): 6.70 (1H, br s, N*H* G_1), 6.45 (1H, br s, N*H* G_2), 4.74 (2H, s, Cp *o*-C*H*), 4.37 (2H, s, Cp *m*-C*H*), 4.24 (5H, s, Cp unsub.), 4.20 (2H, q, $J_{HH} = 7.2$ Hz, $-OCH_2CH_3$), 4.13 (2H, d, $J_{HH} = 5.2$ Hz, CH_2 G_2), 4.06 (2H, d, $J_{HH} = 5.3$ Hz CH_2 G_1), 1.27 (3H, t, $J_{HH} = 7.1$ Hz, $-OCH_2CH_3$). ^{13}C{^{1}H}-NMR (δ in ppm, $CDCl_3$): 171.7, 170.2, 169.9 (C=O), 75.2 (*i*-*C* Cp), 71.0 (2*C*H Cp), 70.1 (*C* unsub. Cp), 68.6 (2*C*H Cp), 61.8 (O*C*H_2), 43.6 (*C*H_2 of G_1), 41.6 (*C*H_2 of G_2), 14.4 (OCH_2CH_3).[1]

2.4.2. Spectroscopic data for Fc–AA–OEt (**5**)

Yield: 63%. Elemental analysis for $C_{24}H_{26}FeN_2O_4$: Anal. Calc. C, 62.35; H, 5.67; N, 6.06. Found C, 62.47; H, 5.47; N, 6.13. ^{1}H-NMR (δ in ppm, $CDCl_3$): 7.68 (1H, d, $J_{HH} = 7.1$ Hz, N*H* A_2), 7.34 (5H, br s, C_6H_5), 6.88 (1H, d, $J_{HH} = 7.7$ Hz, N*H* A_1), 5.17 (2H, quintet, O*C*$H_2C_6H_5$), 4.85 (1H, q, $J_{HH} = 7.2$ Hz, C*H*$^\alpha$ A_1), 4.74 (2H, d, $J_{HH} = 1.6$ Hz, Cp *o*-*H*), 4.59 (1H, p, $J_{HH} = 7.2$ Hz, C*H*$^\alpha$ A_2), 4.34 (2H, d, $J_{HH} = 1.7$ Hz, Cp *m*-*H*), 4.20 (5H, s, Cp unsub.), 1.47 (3H, d, $J_{HH} = 7.3$ Hz, CH_3 A_1), 1.44 (3H, d, $J_{HH} = 7.5$ Hz, CH_3 A_2). ^{13}C{^{1}H}-NMR ($CDCl_3$): 172.9, 172.6 (C=O $A_{1,2}$), 170.5 (C=O Fc), 135.5 (*i*-*C* Bzl), 128.7 (*o*-*C*H Bzl), 128.5 (*p*-*C*H Bzl), 128.2 (*m*-*C*H Bzl), 75.3 (*i*-*C* Cp), 70.8 (*o*-*C*H Cp), 69.9 (*C*H unsub. Cp), 68.4 (*m*-*C*H Cp), 67.1 (O*C*H_2), 48.7, 48.4 (*C*H$^\alpha$ $A_{1,2}$), 19.1 (*C*H_3 A_1), 17.8 (*C*H_3 A_1).

2.4.3. Spectroscopic data for Fc–LF–OMe (**6**)

Yield: 63%. Elemental analysis of $C_{27}H_{32}FeN_2O_4$: Anal. Calc. C, 64.29; H, 6.39; N, 5.55. Found C, 65.24; H, 6.25; N, 5.38. FAB-MS (− ve ion mode): 504.4 $[M^-]$. Accurate mass for $C_{27}H_{32}FeN_2O_4$: Anal. Calc. 504.1711. Found, 504.1706. ^{1}H-NMR (δ in ppm, $CDCl_3$): 7.21 (3H, d, $J_{HH} = 6.7$ Hz, overlapping *m*-C*H* and *p*-C*H* F), 7.11 (2H, d, $J_{HH} = 5.3$ Hz, *o*-C*H* F), 6.57 (1H, d, $J_{HH} = 7.4$ Hz, N*H* F), 6.00 (1H, d, $J_{HH} = 8.1$ Hz, N*H* L), 4.85 (1H, *m*, C*H*$^\alpha$ F), 4.73 (1H, s, *o*-C*H* Cp), 4.64 (1H, s, *o*-C*H* Cp), 4.61 (1H, m, C*H*$^\alpha$ L), 4.39 (2H, s, *m*-C*H* Cp), 4.20 (5*H*, s, unsub. Cp), 3.73 (3H, s, O*C*H_3), 3.12 (2H, m, CH_2 of F), 1.68 (3H, m, CH$^\alpha$*C*H_2*C*H$(CH_3)_2$ L), 0.97 (6H, d, $J_{HH} = 5.8$ Hz, $CH_2CH(CH)_3$ L). ^{13}C{^{1}H}-NMR (δ in ppm, $CDCl_3$): 172.1 (C=O), 171.8 (C=O), 170.7 (C=O Fc), 135.9 (*i*-*C* F), 129.5 (*o*-*C*H F), 128.8 (*m*-*C*H F), 127.3 (*p*-*C*H F), 75.4 (*i*-*C* Cp), 70.9 (*m*-*C*H Cp), 70.0 (*C*H unsub. Cp), 68.8 (*o*-*C*H Cp), 68.1 (*o*-*C*H Cp), 53.6, 52.6, 51.5 (*C*H$^\alpha$ F, *C*H$^\alpha$ L, and O*C*H_3), 41.4, 38.1 [$-$*C*H_2CH$(CH_3)_2$ L, and $-$*C*$H_2C_6H_5$ F], 25.1 (*C*HCH$_3$ L), 23.2 (CH*C*H$_3$ L), 22.3 (CH*C*H$_3$ L).

[1] G_1 = N-terminal residue; G_2 = C-terminal residue.

Table 1
Association constants (K_A), and Redox potentials ($E_{1/2}$ in mV) and peak separation (mV) of ferrocenoyl-peptides **2**–**4** before and after the addition of one equivant of APzl

Compound	K_A (M^{-1})	$\Delta E_{1/2}$ (mV)[a]	
		–	APzl (**8**)[b]
Fc–G_2–OEt (**2**)	9.4 ± 1.0	147 ± 2 (83)	146 ± 2 (91)
Fc–A_2–OBzl (**3**)	12.7 ± 1.4	146 ± 2 (70)	133 ± 2 (69)
Fc–LF–OMe (**4**)	21.4 ± 0.5	148 ± 2 (104)	118 ± 2 (124)

[a] Potentials are measured vs. ferrocene/ferrocenium redox couple in 0.1 M TBAP in dry $CHCl_3$ solution, scan rate = 100 mV s^{-1}.

[b] Scanned only up to 0.8 V vs. Ag/AgCl due to polymerization of APzl, which causes a surface modification of the working electrode

2.5. ^{1}H-NMR titration experiments

2.5.1. Titrations

From a stock solution of Fc-peptide in $CDCl_3$, a dilute sample of Fc-peptide is prepared (ca. 5.9 mM). An initial spectrum is collected, then portions of APzl from a stock solution (0.18 M), are added via microsyringe (10 & 50 μl, Hamilton; 500 μl, SGE). After each addition the sample is shaken vigorously, injected into the spectrometer, and allowed to spin for at least 10 min in order to thoroughly mix the solution. The amide protons of Fc-peptide are monitored and the chemically induced shift (CIS) is plotted vs. the mole ratio of APzl to Fc-peptide. The association constants (K_A) for the interaction as well the saturation point, where full complexation of Fc-peptide by APzl occurs, is determined by non-linear regression (vide infra).

2.5.2. Job plots

Equimolar stock solutions of Fc-peptide and APzl (1 M) in $CDCl_3$ were prepared and then mixed to provide a series of 10 samples of varying mole fractions (X). A total of 250 μl of $CDCl_3$ was added to each NMR tube in order to give an acceptable sample volume. Chemical shifts of amide protons were monitored as a function of X of the host Fc-peptide. The change in chemical shift ($\Delta\delta$) multiplied by X of host was plotted versus X of host according to Job's method of continuous variation [16] modified for NMR by Blanda et al [11]. The stoichiometry of the resulting complex is obtained from the Job plot by observing the positions of the maxima in the curve, where a maximum at $X = 0.5$ corresponds to a complex with 1:1 stoichiometry.

2.5.3. Association constants

K_A for **2**–**4** with APzl are listed in Table 1, and are determined by a non-linear curve fitting procedure using SIGMAPLOT[2], using a two state (1:1) binding model as

[2] SIGMAPLOT version 4.0 (1995) is available from Labtronics, 95 Crimea St., Guelph, Ont N1H 2Y5, Canada. Tel.: + 1-519-767-1061.

defined by Eqs. (1) and (2), where [Fc-peptide·APzl], [Fc-peptide], and [APzl] refer to the equilibrium concentrations of each species. An appropriate derivation of the equations used in the regression is given in Appendix 1 [16].

$$\text{APzl} + \text{Fc-peptide} \rightleftharpoons \text{Fc-peptide} \cdot \text{APzl} \quad (1)$$

$$K_A = \frac{[\text{Fc-peptide} \cdot \text{APzl}]}{[\text{Fc-peptide}] \cdot [\text{APzl}]} \quad (2)$$

2.5.4. Electrochemistry

All electrochemical experiments were carried out in air at room temperature (21 ± 2°C) on a BAS CV-50 Voltammetric Analyzer. The solvent was $CHCl_3$ containing 0.1 M tetrabutylammonium perchlorate (TBAP) as supporting electrolyte. For the cyclic voltammetry studies a glassy carbon working electrode (diameter 3 mm) and a platinum wire counter electrode were used. The reference electrode was a Ag/AgCl electrode. iR compensation was applied. Backgrounds of the solvent containing 0.1 M TBAP were collected before each set of experiments and then subtracted from the spectra. Stock solutions of Fc-peptide (0.012 M) and APzl (0.061 M) in $CHCl_3$ were used. A total volume of 100 μl of the peptide solution was added to 3 ml of 0.1 M TBAP solution via microsyringe (250 μl, Hamilton). Initially, a voltammogram was collected from 0 to 1000 mV (vs the Ag/AgCl electrode) at a scan rate of 100 mV s^{-1} and then narrowed to a scan range of 800 mV. One equivalent of APzl solution was then added and a voltammogram collected. A second CV spectrum was recorded after a second equivalent of APzl was added.

3. Results and discussion

All Boc-peptide esters were obtained in high yields by the standard HOBt/DCC protocol. Ferrocenecarboxylic acid (**1**) is cleanly coupled to C-protected peptide esters under basic peptide coupling conditions to give orange to yellow Fc-peptide esters (Fc–G_2–OEt (**2**), Fc–A_2–OBzl (**3**), Fc–LF–OMe (**4**)) (A = alanine, Ala; G = glycine, Gly; L = leucine, Leu; F = phenylalanine, Phe).

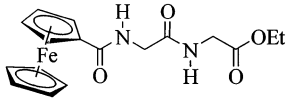

Fc-G_2-OEt, **2**

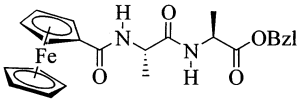

Fc-A_2-OBzl, **3**

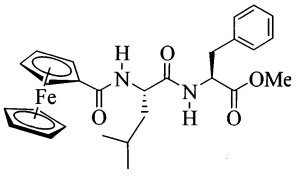

Fc-LF-OMe, **4**

These crystalline solids are highly soluble in most organic solvents. The synthesis of Fc–G_2–OEt (**2**), representative of **2**–**4** is shown in Scheme 2.

The ^{1}H-NMR spectra of all three peptides exhibit the typical signal pattern for monosubstituted ferrocenoyl systems, having the ortho protons of the substituted

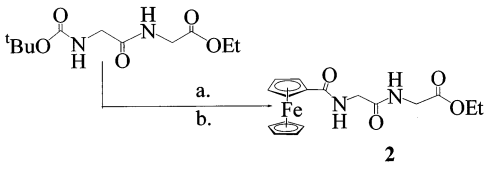

Scheme 2. Synthesis of Fc–G_2–OEt (**2**). (a) TFA, CH_2Cl_2, 30 min; then Et_3N. (b) Ferrocene–carboxylic acid/DCC/HOBt/CH_2Cl_2, 12 h at room temperature.

Cp ring downfield from the meta protons [6]. For **2** and **3**, only singlets are observed for the ortho protons. Only for **4** is it possible to resolve the two enantiotopic ortho protons and two singlets are observed at δ 4.73 and 4.64. All systems give rise to two distinct amide resonances, which are highly concentration dependent.

The H-bonding interaction between the amide H of Fc-peptides **2**–**4** and substrates such as substituted pyrazoles, causes shifts in the peak positions of the Fc-peptide amide protons, and can be coveniently followed by ^{1}H-NMR spectroscopy.

Initially, we started investigating the interaction of simple Fc–amino acids, such as Fc–G–OEt and Fc–A–OBzl with pyrazole. In ^{1}H-NMR titration experiments, we observed only small chemically induced shifts (CIS) of their amide resonances, indicating that only a weak two-point hydrogen bonding interaction exists [9b], giving rise to 1:1 complexes in each case (Scheme 3). This is in agreement with Schrader's results [9].

The crystal structures of other Fc-amino acid systems clearly show that the amido function of the molecule lies coplanar to the Cp ring, a conformation, which is preserved amongst most Fc systems [6,7,12]. This conformation allows only the carbonyl group of the ester, and not the Fc C=O, to interact with pyrazole in a two-point binding mode as indicated in Scheme 3. Next we investigated the interaction of APzl with Fc-peptide esters **2**–**4** by NMR spectroscopy. Upon addition of APzl to solution of Fc-peptide in $CDCl_3$, both amide protons exhibit

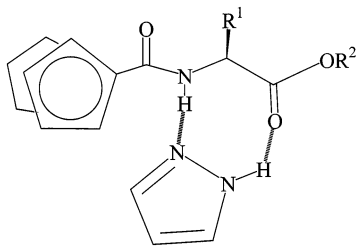

Scheme 3. Interaction of Fc-amino acids (Fc–A–OBzl, R_1 = Me, R_2 = Bzl; Fc–G–OEt, R_1 = H, R_2 = Et) with pyrazole. One pyrazole molecule forms two dynamic hydrogen bonds with Fc-amino acids.

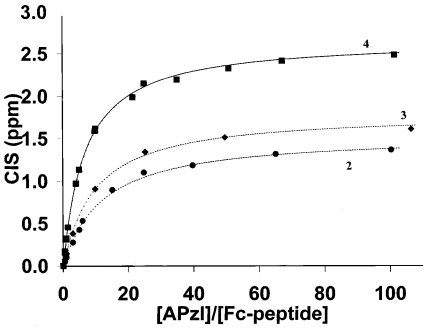

Fig. 1. Interaction of APzl with Fc-peptides **2**–**4**. Shown are the changes in δ (in ppm) for the C-terminal amide proton which take place upon addition of APzl to a solution of Fc-peptide in $CDCl_3$. The amide proton interacting more strongly with the APzl exhibits the larger change in δ: ■ amide of the phenylalanine residue of **4**; ● amide of the C-terminal glycine residue of **2**; ◆ amide of the C-terminal alanine residue of **3**. Non-linear regression curve fits are plotted for each system.

large downfield shifts from their initial positions. Fig. 1 shows the CIS of one of the amides of Fc-peptides **2**–**4** upon addition of APzl. From this we obtained association constants (K_A) by non-linear regression (see experimental, Appendix 1). Table 1 summarizes K_A for the interaction of APzl with the top face of Fc-peptides **2**–**4**.

It is noticable that **2** exhibits the weakest K_A for the interaction with APzl ($9.4 \pm 1.0\ M^{-1}$). This is in accordance with what Schrader observed for pyrazole binding to N,C-protected dipeptides containing glycine [9]. In Schrader's systems, K_A's were 3 to 4 times smaller in glycine containing peptides than in glycine-free peptides [9b]. This arises due to the fact that G residues are highly flexible since they have no sidechain to restrict rotation around the bonds of the α-carbon, and is an indication that **2** is not ideal for interaction with APzl. The presence of the amino acid sidechains in **3** and **4** restricts the flexibility of the peptide backbone compared to **2** and also makes the approach for APzl to the Fc-peptide more restricted. In this context it is of interest to investigate systems with an inherent preference for the β-sheet conformation, such as leucine- and phenylalanine-containing peptides and compare them to systems that lack this preference, such as oligoalanines [13].

In **4** the sterically demanding side chains are already favouring the β-sheet conformation [13]. Hence, differentiation between the stronger and weaker binding modes (three-point vs. two-point binding) should not only be possible in these systems, but should be stronger for **4**. Hence, we monitored the interaction of **3** and **4** with APzl by ^{1}H-NMR spectroscopy and observed large downfield CIS of the amide protons of up to 2.5 ppm. Expectedly, the interactions are the strongest for **4** with APzl. The interaction of the F amide is stronger than that of the L amide, indicating that there is a preference for complexation to the C-terminal F residue. Using the CIS information, we constructed pseudo-Job plots ($\Delta\delta X_{\text{Fc-peptide}}$ vs. $X_{\text{Fc-peptide}}$) [11] for the interaction of all three Fc-peptides with APzl, which allowed us to obtain the approximate stoichiometries of the adducts. Such a plot for the

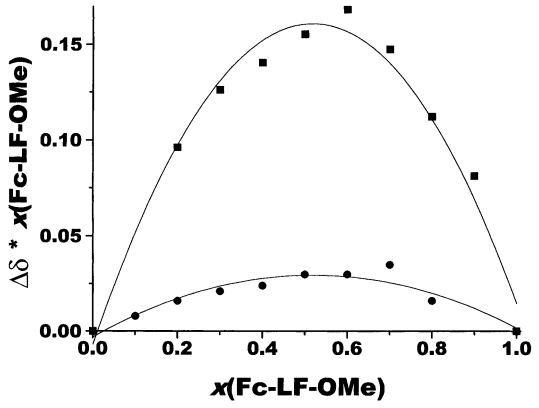

Fig. 2. Pseudo-Job plot for the interaction of APzl with **4**: ■ phenylalanine (F) amide; ● leucine (L) amide.

interaction of **4** with APzl is presented in Fig. 2. The Job plot [11] for the interaction of APzl with the F amide is significantly more intense than that of the L amide, giving a strong maximum at a 1:1 stoichiometry. Likewise, the L amide has a very weak maximum also at 1:1 stoichiometry. We want to stress that the results obtained from a pseudo-Job method cannot unequivocally prove 1:1 binding, but should only be used as an indication that the top face interacts preferentially with APzl (Scheme 4). In order to establish the overall binding stoichiometry, we carried out non-linear regressions of our NMR titration data for all systems investigated, described in detail in the experimental section. For all systems, we were able to fit our NMR data to a two state model (see Eq. (1)) giving a 1:1 stoichiometry exclusively. We have no evidence to support the formation of a 1:2 complex in solution. For the interaction of **4** with APzl a K_A of $21.4 \pm 0.5\ M^{-1}$ was obtained. This is the highest K_A observed for any of the three Fc-peptides investigated. Due to the inherent preference of L and F-containing peptides to exist in the extended conformation [13], we expected Fc–LF–OMe to exhibit the strongest interaction with APzl. Our observations are not unlike Schrader's results,

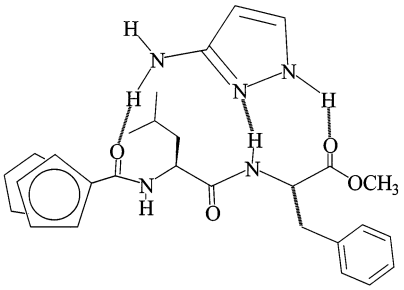

Scheme 4. Shown is the interaction of 3-aminopyrazole (APzl) with Fc–LF–OMe (**4**). One APzl molecule interacts with **4** by forming three hydrogen bonds with the peptide backbone.

who has observed stronger binding of dipeptides with APzl which prefer the extended conformation [9]. It is important to point out at this point that the two methyl groups of the L residue in **4**, which are magnetically identical in the uncomplexed state and give rise to a doublet at δ 0.97, become magnetically inequivalent upon addition of APzl. In the **4**/Apzl complex, they give rise to two doublets at δ 0.93 and 0.90. This clearly demonstrates that the movement of the *i*-Pr group is restricted upon addition of APzl, similar to the restricted movement that was observed in glycine containing dipeptides [9b].

We conclude that the interaction of APzl is significantly stronger and more specific for **4** than it is for the interaction with **2** and **3**. At this point we can only assume that this behavior is related to the preorganization of the Fc-peptides and the preference of peptides containing certain amino acids that have a high propensity for forming β-sheets. This is most likely the case for **4** and hence conformational changes that contribute to the activation barrier for β-sheet formation will be small for the interaction of **4** with APzl compared to the diglycine and dialanine systems, which do not have the inherent tendency to form β-sheets. In these systems, conformational changes are significantly larger and lead to a decrease in the stability of the complex.

In order to determine the extent of H-bonding in the **4**/APzl complex, we carried out a variable temperature ^{1}H-NMR study of **4** in the presence of one equivalent of APzl below self-association concentration. For peptides below self-association concentration, the temperature dependence of the amide resonances is usually small (-2 to -4 ppb K^{-1}) [9b,14,15]. Thus, any temperature effects that are observed must be related to the interaction of the Fc-peptide with APzl. In our VT study of a 1:1 solution of **4** and APzl, the F amide proton has the same chemical shift as the aromatic hydrogens at 298 K (δ 7.19) but separates from them at elevated temperatures. At 338 K the resonance is found upfield at δ 6.91 which is a temperature dependence of -7 ppb K^{-1}. This is perhaps not a strong temperature dependence. But in sharp contrast, the L amide proton barely changes from its initial position at δ 6.11, showing a temperature dependence of less than -1 ppb K^{-1}. Hence, the observed temperature behavior of the F and L amides is further proof that APzl is able to recognize the top face of **4**.

Next, we studied the electrochemical behavior of the Fc-peptides **2**–**4** in $CHCl_3$ in the presence and absence of APzl, using cyclic voltammetry Table 1). The voltammograms for **2**–**4** exhibit fully reversible one-electron oxidations as expected for Fc systems. As observed before for ferrocenoyl amino acids [6], we observe only slight variations in the oxidation potentials on changing the peptide from G_2 to A_2 to LF. The redox potentials of the unbound Fc-peptides are very similar ($E_{1/2} = 146 \pm 2$ mV versus the ferrocene/ferrocenium$^+$couple). Addition of APzl to solutions of Fc-peptides **2**–**4** causes shifts in the redox potentials of **3** and **4**. For **4**, the potential shifts by 30 mV from 148 to 118 mV (vs. ferrocene/ferrocenium) as shown in Fig. 3. ^{1}H-NMR measurements have confirmed that complex formation takes place by binding of APzl to the top face of the Fc-peptide backbone of **4**. In contrast to that, no change in the redox potential is observed for **2**, and **2** exhibits the weakest binding of the three Fc-peptides to APzl. Being intermediate in its interaction with APzl, **3** exhibits a shift of 13 mV upon complexation. Addition of

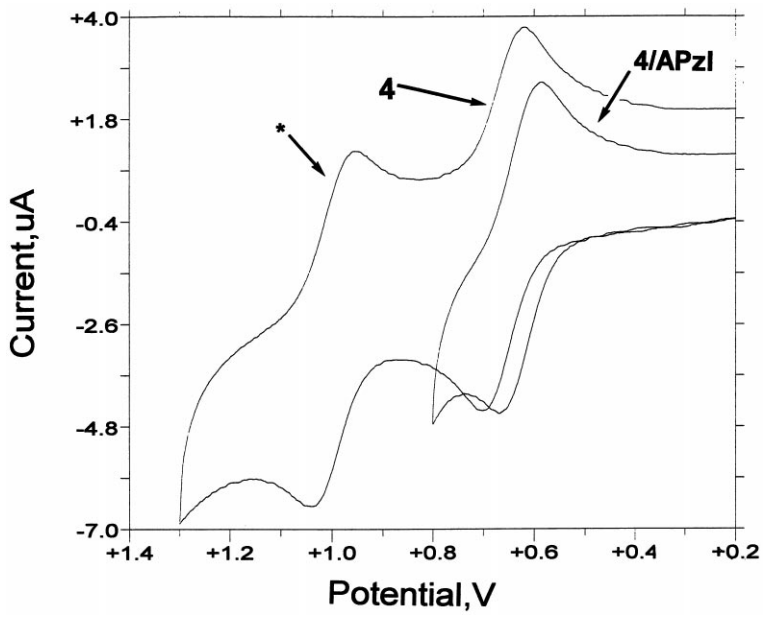

Fig. 3. Cyclic voltammogram for **4** in the absence and presence of APzl in $CHCl_3$ with 0.1 M tetrabutylammonium perchlorate (TBAP) as supporting electrolyte (glassy carbon working electrode, Pt wire counter electrode and a Ag/AgCl reference electrode; 100 mV s^{-1}). The presence of 1,1′-diacetylferrocene as internal standard in the initial scan is denoted by '*'.

a second equivalent of APzl (and even excess) does not cause any further changes in the redox potential of the Fc moiety in **2**–**4**. This is in line with our NMR titration experiments which indicate a 1:1 stoichiometry only for all complexes.

Addition of APzl also causes a change in the capacitance current (Fig. 3). This is due to the modification of the electrode due to polymerization of APzl (at ca. 0.9 V vs. Ag/AgCl). We are currently exploring this issue further.

4. Summary

Our electrochemical results are in agreement with the NMR measurements of the interactions of the Fc-peptides with APzl, which show that the strength of the β-sheet forming interaction of APzl with Fc-peptide increases in the order $\mathbf{2} < \mathbf{3} \ll \mathbf{4}$. Our results demonstrate that the Fc moiety is sensitive to binding of APzl to the Fc-peptide. It is important to stress that the interaction of APzl with the Fc-peptides stabilizes the Fe(III) state of the ferrocenoyl moiety more than helical oligoprolines [7]. However, at present it is not possible to quantitatively relate any changes in potential to the conformation of the peptide due to the lack of a large database which will be necessary in order to draw decisive conclusions. We are continuing to design Fc-peptides as well as pyrazole derivatives in order to optimize

their ability to act as β-sheet models which will be used in future electron transfer measurements.

Acknowledgements

The authors would like to thank Dr R.S. Reid of the Department of Chemistry at the University of Saskatchewan for his expert advice with non-linear regression. This work was supported in part by the Samuel and Ethel Brown Memorial Fund and the Department of Chemistry, U. of S. H.-B.K. is recipient of the University of Saskatchewan NSERC President's Award.

Appendix 1. Derivation of SIGMAPLOT regression equation

Substitution of Eqs. (3)–(5) into Eq. (2) and subsequent algebraic manipulation yields the quadratic Eq. (6):

$$[\text{Fc-peptide} \cdot \text{APzl}] = \alpha_{\text{Fc-peptide} \cdot \text{APzl}^*}[\text{Fc-peptide}]_o \tag{3}$$

$$[\text{Fc-peptide}] = \alpha_{\text{Fc-peptide}^*}[\text{Fc-peptide}]_o \tag{4}$$

$$[\text{APzl}] = [\text{APzl}]_o - [\text{Fc-peptide} \cdot \text{APzl}] \tag{5}$$

where $[\text{Fc-peptide}]_o$ and $[\text{APzl}]_o$ refer to the total concentration of each species, and $\alpha_{\text{Fc-peptide}}$ and $\alpha_{\text{Fc-peptide·APzl}}$ correspond to the fractions of free and bound Fc-peptide at equilibrium:

$$\alpha_{\text{Fc-peptide}} = \frac{[\text{Fc-peptide}]}{[\text{Fc-peptide}]_o} = \frac{-b + (b^2 + 4a)^{1/2}}{2a} \tag{6}$$

where $a = K_{A^*}[\text{Fc-peptide}]_o$ and $b = (K_{A^*}[\text{APzl}]_o - K_{A^*}[\text{Fc-peptide}]_o) = 1$.

The observed chemical shift (δ) is a time averaged signal, due to fast exchange on the NMR time scale, which gives the relationship in Eq. (7).

$$\delta_{obs} = \alpha_{\text{Fc-peptide}^*}\delta_{\text{Fc-peptide}} + \alpha_{\text{Fc-peptide} \cdot \text{APzl}^*}\delta_{\text{Fc-peptide} \cdot \text{APzl}} \tag{7}$$

Since we use CIS ($\Delta\delta_{obs}$) as opposed to absolute chemical shifts, $\delta_{\text{Fc-peptide}} = 0$ and $\alpha_{\text{Fc-peptide}^*}\delta_{\text{Fc-peptide}}$ reduces to zero leaving Eq. (8), where $\Delta\delta_{\max} = \delta_{\text{Fc-peptide·APzl}}$:

$$\Delta\delta_{obs} = \alpha_{Fc-peptide^*APzl^*}\Delta\delta_{\max} \tag{8}$$

Finally, substitution of $\alpha_{\text{Fc-peptide·APzl}} = 1 - \alpha_{\text{Fc-peptide}}$ into Eq. (8) gives the equation used for the SIGMAPLOT regression [$\delta_{obs} = (1 - \alpha_{\text{Fc-peptide}})\Delta\delta_{\max}$].

References

[1] P.D. Beer, Chem. Soc. Rev. 18 (1989) 409.
[2] P.D. Beer, Z. Chen, A.J. Goulden, A. Graydon, S.E. Stokes, T. Wear, J. Chem. Soc. Chem. Commun. (1993) 1834.

[3] P.D. Beer, Z. Chen, M.G.B. Drew, J. Kingston, M. Ogden, P. Spencer, J. Chem. Soc. Chem. Commun. (1993) 1046.
[4] Z. Chen, A.R. Graydon, P.D. Beer, J. Chem. Soc. Faraday Trans. 92 (1996) 97.
[5] E.C. Constable, Angew. Chem. Int. Ed. Engl. 30 (1991) 407.
[6] H.-B. Kraatz, J. Lusztyk, G.D. Enright, Inorg. Chem. 36 (1997) 2400.
[7] H.-B. Kraatz, A. Houmam, D.M. Leek, G.D. Enright, J. Lusztyk, D.D.M. Wayner, J. Organomet. Chem 589 (1999) 42.
[8] J.P. Schneider, J.W. Kelly, Chem. Rev. 95 (1995) 2169–2187.
[9] (a) T.H. Schrader, C.N. Kirsten, J. Chem. Soc. Chem.Commun. (1996) 2089. (b) C.N. Kirsten, T.H. Schrader, J. Am. Chem. Soc. 119 (1997) 12061.
[10] S.I Goldberg, L.H. Keith, T.S. Prokopov, J. Org. Chem. 28 (1963) 850.
[11] M.T. Blanda, J.H. Horner, M. Newcomb, J. Org. Chem. 54 (1989) 4626.
[12] L. Lin, A. Berces, H-B. Kraatz, J. Organometal. Chem. 556 (1998) 11.
[13] C.K. Smith, L. Regan, Acc. Chem. Res. 30 (1997) 153.
[14] J.S. Nowick, E.M. Smith, J.G. Noronha, J. Org. Chem. 60 (1995) 7386.
[15] J.S. Nowick, D.L. Holmes, G. Mackin, G.J. Noronha, A.J. Shaka, E.M. Smith, J. Am. Chem. Soc. 118 (1996) 2764.
[16] K.A. Connors, Binding Constants: The Measurement of Molecular Complex Stability, Wiley-Interscience, New York, 1987, pp. 24–28.